Journal of Visualization, Vol. 4, No. 3 (2001) 211

Visualization of Plane Free Jet Impinging on the Edge

Fujisawa, N.[1] and Takizawa, Y.[2]

1) *Department of Mechanical and Production Engineering, Niigata University, 8050 Ikarashi 2, Niigata 950-2181, Japan*

2) *Graduate School of Science and Technology, Niigata University, 8050 Ikarashi 2, Niigata 950-2181, Japan*

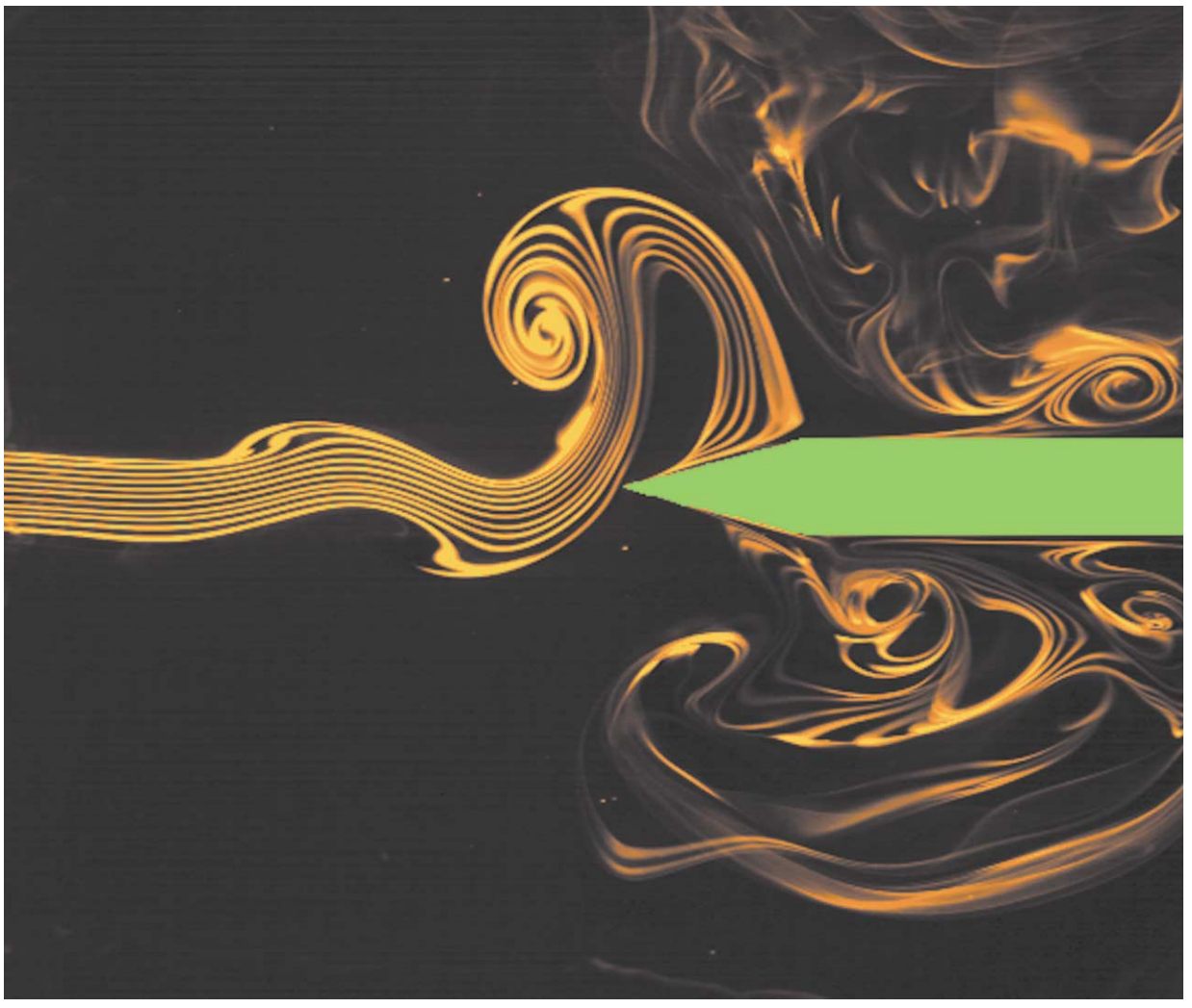

This picture shows the interaction of the plane free jet and the edge, which is visualized by the dye injection technique with a dilute Rhodamine B solution. The experiment is carried out in a water tunnel at Re (=Ud/ν)= 430, which is defined by the jet flow velocity U and the height d of the jet nozzle. The edge apex is located at x/d=8 from the nozzle exit. The flow field around the edge indicates the appearance of frequency jump in flow oscillation in front of the edge and further amplification of the vortices in the downstream.

Journal of Visualization, Vol. 4, No. 3 (2001) 212

Visualization of Vapour Bubble Growth

***Kowalewski, T.A.*[1)]*, Pakleza, J.*[2)]*, Chalfen, J.-B.*[2)]*, Duluc, M.-C.*[2)] *and Cybulski, A.*[1)]

1) *Polish Academy of Sciences, IPPT PAN, Swietokrzyska 21, PL-00049 Warsaw, Poland*

2) *LIMSI-CNRS, F- 91403 Orsay Cedex, France*

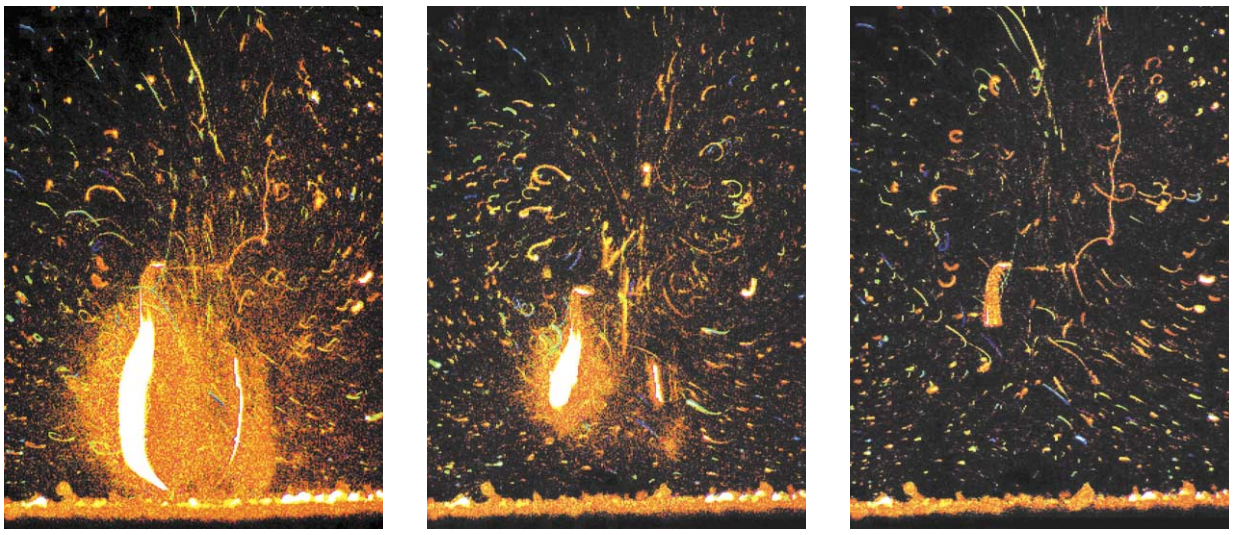

(a) (b) (c)

Figure 1

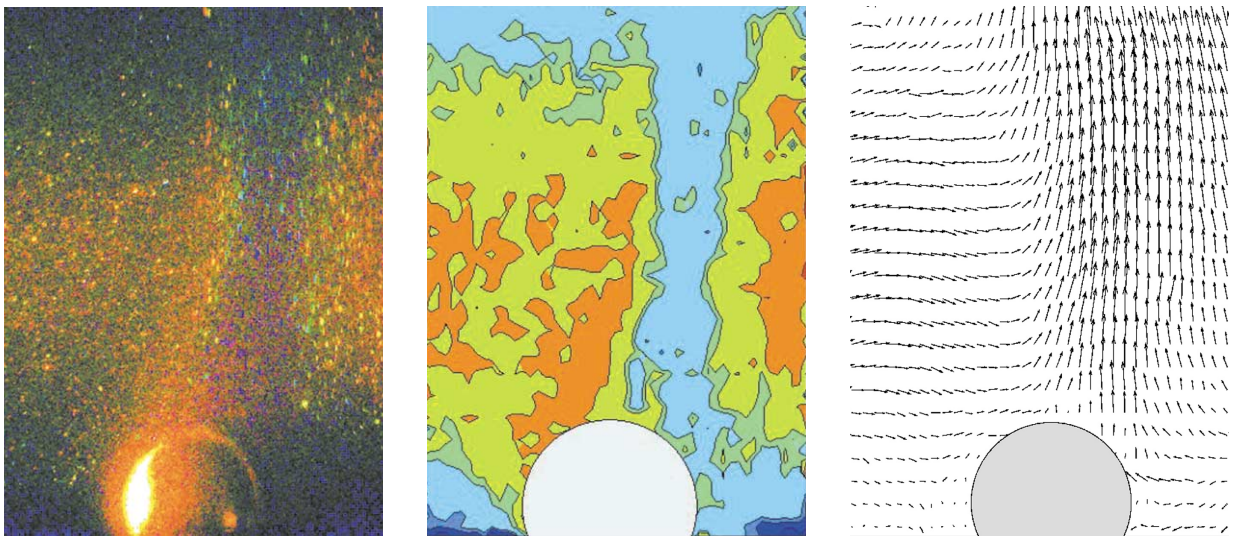

(a) (b) (c)

Figure 2

The growth of a single microscopic water vapour bubble under low-pressure condition at the heated surface was investigated experimentally. The flow was seeded with thermochromic liquid crystals. Both velocity and temperature fields surrounding the bubble are evaluated using Particle Image Velocimetry and Thermometry method. Figure 1 shows flow field associated with departure and implosion of the vapour bubble. The light sheet technique is used; hence only reflections from the bubble surface can be seen here. The exact bubble form was recorded from the perpendicular direction using bright field illumination. Long illumination time (20 ms) is used to visualize complexity of the flow structure. Variation of the tracer colour demonstrates non-uniformity of the instantaneous temperature field. After implosion (Fig. 1(c)) few remaining tiny satellite bubbles moving away with a velocity of few m/s can be seen. Figure 2 illustrates (a) flow field surrounding the steady vapour bubble visualized with liquid crystal tracers, (b) the evaluated temperature field and (c) the corresponding velocity field. The experimental conditions are: pressure - 6.1kPa, liquid temperature - 35.7˚C, heated wall temperature - 57˚C.

Journal of Visualization, Vol. 4, No. 3 (2001) 213

Wake Structure of Bubbly Flows around Various Types of Objects

Fujimoto, K.[1)], Ishikawa, M. [2)], Minami, T.[2)], Murai, Y. [2)],and Yamamoto, F.[2)]

1) *Applied Business Studies, Kinjo College, 1200 Kasama-machi, Matto, Ishikawa 924-8511, Japan*

2) *Department of Mechanical Engineering, Fukui University, 3-9-1 Bunkyo, Fukui 910-8507, Japan*

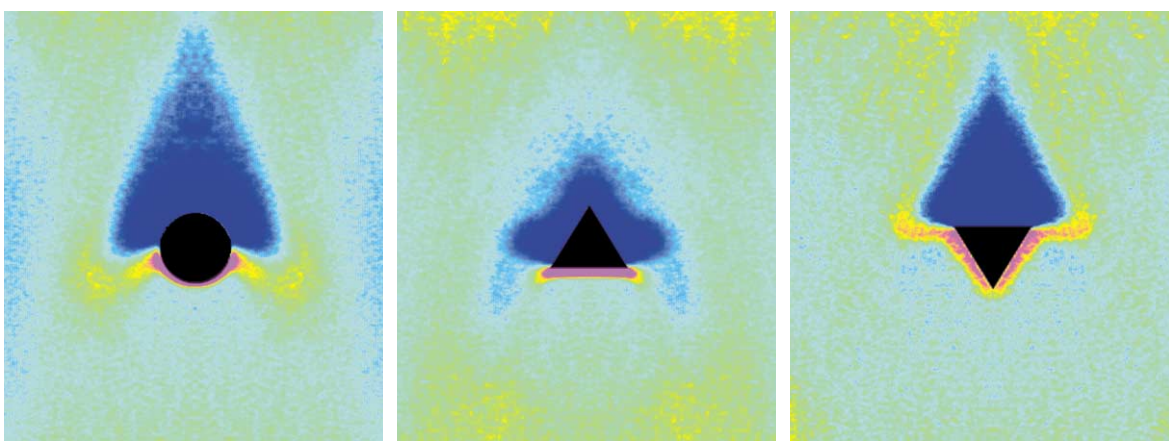

(a) Circular cylinder

(b) Triangular cylinder (Plane-counter)

(c) Triangular cylinder (Edge-counter)

(d) Square cylinder (Plane-counter)

(e) Square cylinder (Edge-counter)

Local void fraction distribution due to various shapes of objects.
Void fraction $\alpha = 0.074$, Bubble radius $r_g = 1.76$ mm.

When a solid object is put in a free-rising bubble flow, a large convection is induced around the object. The convection scale is much greater than the length scale of the object, which is never seen in incompressible single-phase flow. This phenomenon is clearly observed when the bubbly flow is formed in a small channel and has equaled bubble size as well as spatially uniform void fraction in the upstream of the object. Detailed specification is as follows. Coaxial twin rectangular chamber made of transparent acrylic resin is used, which is 500 mm in width and 1000 mm in height. The channel depth is 10 mm. 376 bubble injection nozzles with ID of 0.3 mm are installed on all four channels. Room temperature air is supplied from the compressor through a high accuracy pressure controller and flow meter. A back lighting method through an irradiating metal halide lamp (250w$\times$two), which is set in the central cavity of the chamber is adopted in order to get the bubble shadow image. An optical diffusion sheet is also supplemented. A flow field of 0.50 m$\times$0.50 m surrounding the object is recorded by a digital video camera. The pictures show the local void fraction distribution in the case that void fraction $\alpha = 0.074$ and bubble radius $r_g = 1.76$ mm.

Journal of Visualization, Vol. 4, No. 3 (2001) 214

Animation Understanding of Inclined Bluff Body Flows by Multi-vision PIV*

***Lee, Y.-H.*[1)], *Nam, C.-D.*[2)], *Choi, J.-W.*[3)] *and Lee, H.*[3)]**

1) *Division of Mechanical & Information Engineering, Korea maritime University (KMU) 1 Dongsam-dong Youngdo-ku, Busan 606-791, Korea*

2) *Division of Marine System Engineering, KMU, 1 Dongsam-dong Youngdo-ku, Busan 606-791, Korea*

3) *Image Information Technology Co., Ltd., DINTEC Bldg., 1144-10, Choryang 3-dong, Dong-ku, Busan 601-013, Korea*

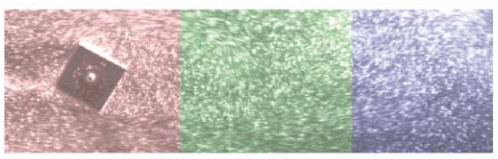

Original image

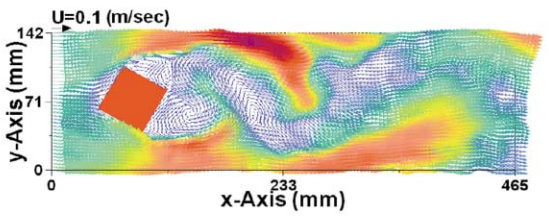

Velocity vectors

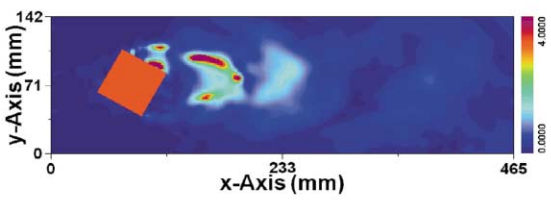

Turbulent intensity

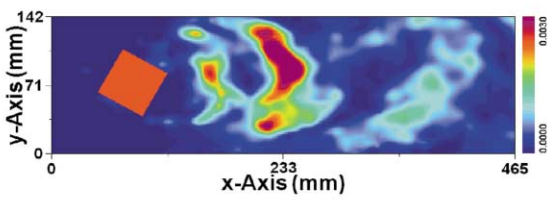

Reynolds stress (- ρ (u')2)

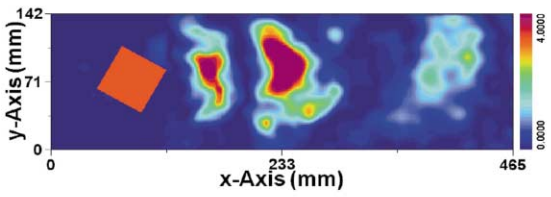

Reynolds stress (- ρ $(v')^2$)

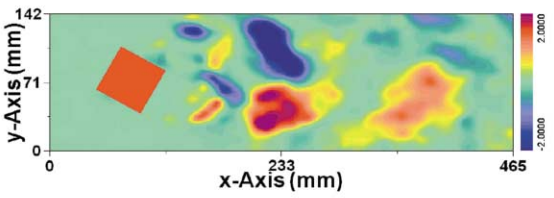

Reynolds stress (- ρ u'v')

Macroscopic understanding and time-resolved analysis of the wake characteristics of 2-D bluff body flows are shown by applying the multi-vision PIV to square cylinders (angle of attacks: 30°) and by the subsequent animation procedures developed originally by the author's group. The experimentation was carried out within a circulating water channel (representative height is 50 mm, Re=104). Three CCD cameras were used to picture the enlarged wake flow field.

* Young-Ho Lee, Chung-Do Nam, Jang-Woon Choi and Hyun Lee, Animation Understanding of 2-D Simple Bluff Body Flows by Multi-vision PIV, Proc. of 9th Int. Symp. on Flow Visualization Paper No. 187, Edinburgh 2000.

Journal of Visualization, Vol. 4, No. 3 (2001) 215

Dye Interaction with Rising Bubbles in a Crossflow

***Crepeau, J. C.*[1)] *and McIlroy, Jr., H. M.*[1)]**

1) *Department of Mechanical Engineering, University of Idaho, P.O.Box 50776, Idaho Falls, Idaho 83405, USA*

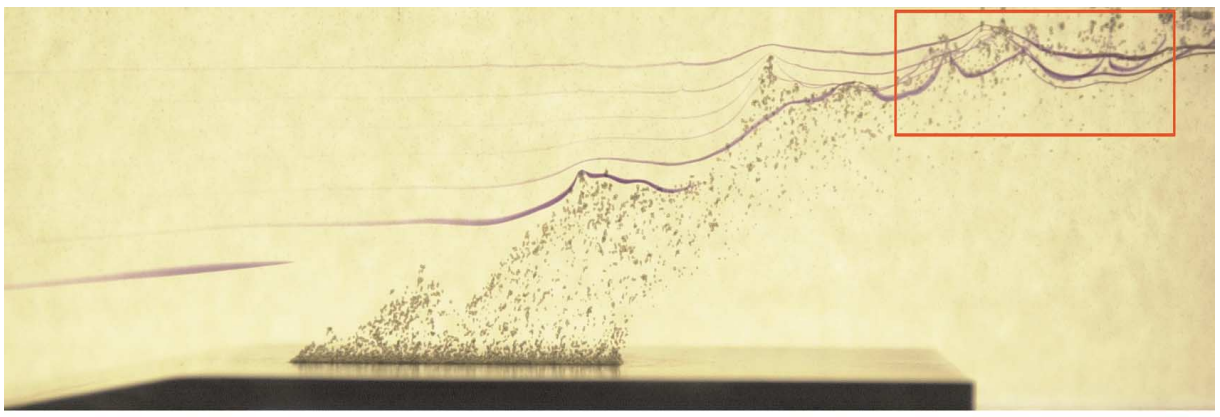

The figure shows the interaction between rising bubbles and dye injected upstream. The bubbles are created by a reaction between the working fluid (a mixture of hexanoic acid and mineral oil) and sodium embedded in a nonreacting metal plate. The Reynolds number is 350, based on the length of the duct. Along the leading edge of the bubbles, one observes a billowing effect, due to the deformation of the boundary layer profile caused by the rising bubbles and the subsequent growth of the Kelvin-Helmholtz instability. In the closeup, the bubbles interact both in groups and individually with the dye filaments. This work was funded by a grant from the U.S. Department of Energy, Environmental Management Science Program.

Journal of Visualization, Vol. 4, No. 3 (2001) 216

Time-resolved PIV Measurement of Three-dimentional Cylinder Wake

***Sung, J.*[1] *and Yoo, J. Y.*[1]**

1) *School of Mechanical and Aerospace Engineering, Seoul National University, Seoul 151-742, Korea*

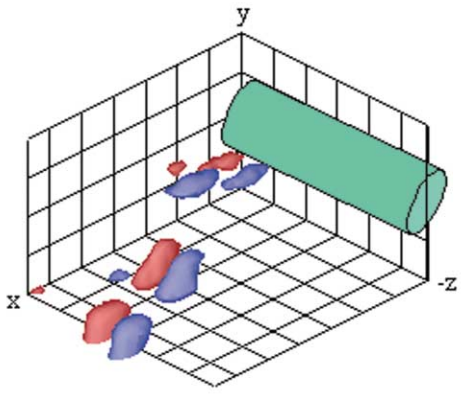

Iso-vorticity (ω_y) surfaces

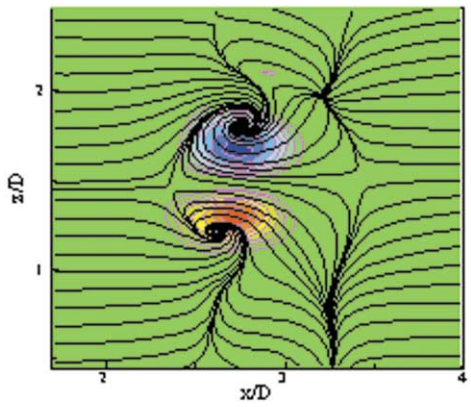

Mushroom-type structure

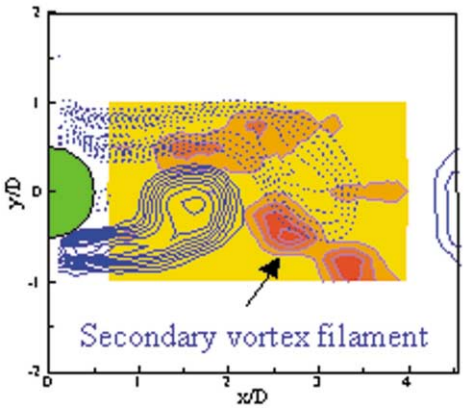

Phase-locked primary and secondary vortices

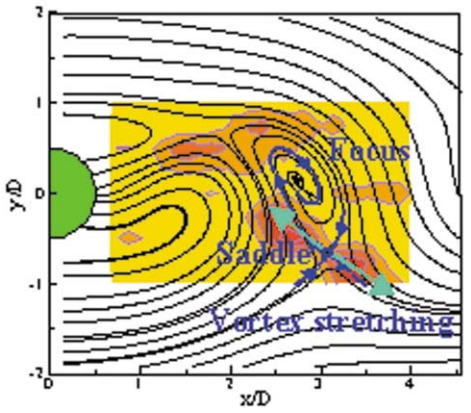

Flow topology around a saddle

Phase-averaged three-dimensional near wake behind a circular cylinder in the wake-transition regime of Reynolds number 360 was measured by a time-resolved PIV system. The upper-left figure shows iso-vorticity surfaces of secondary vortices (ω_y), which were reconstructed from the phase-averaged vorticity fields on several z-x planes. Sectional streamlines around the secondary vortices in the upper-right figure were obtained by subtracting convection velocity, which gives a good evidence for the mushroom-type structure. In the lower two figures, the primary flow in a moving frame of reference was overlapped with the x-y plane view of the secondary vortices. Their spatial dispositions and vortex stretching process can be explained well.